Journal of Nuclear Medicine, published on September 22, 2016 as doi:10.2967/jnumed.116.178707

Parametric methods for dynamic ^{11}C-Phenytoin PET studies

Syahir Mansor[1*], Maqsood Yaqub[1], Ronald Boellaard[1,2], Femke E Froklage[1,3,4], Anke de Vries[1†], Esther DM Bakker[1], Rob A Voskuyl[3], Jonas Eriksson[1‡], Lothar A Schwarte[5], Joost Verbeek[1], Albert D Windhorst[1], Adriaan A Lammertsma[1]

[1]Department of Radiology & Nuclear Medicine, VU University Medical Center, Amsterdam, the Netherlands

[2] Department of Nuclear Medicine and Molecular Imaging, University Medical Center Groningen, University of Groningen, Groningen, the Netherlands

[3]Department of Neurology, Stichting Epilepsie Instellingen Nederland (SEIN), Heemstede, the Netherlands

[4]Department of Neurology, VU University Medical Center, Amsterdam, the Netherlands

[5]Department of Anaesthesiology, VU University Medical Center, Amsterdam, the Netherlands

[*]Corresponding author:

Syahir Mansor, MSc

Department of Radiology & Nuclear Medicine, VU University Medical Center

PO Box 7057, 1007MB Amsterdam, the Netherlands

Telephone: +31 (02)0 4441524

E-mail: m.mansor@vumc.nl

†The author is currently at the Department of Medical Physics, Catharina Hospital Eindhoven, Eindhoven, the Netherlands.

‡The author is currently at the PET Center, Uppsala University Hospital, Uppsala, Sweden.

Source of support:

This work was supported by the European Union seventh framework program EURIPIDES (FP7/2007-2013 under grant agreement no 201380). Syahir Mansor is a PhD student and was supported by a scholarship from the Malaysian Ministry of Education and University Sains Malaysia.

Word count: 3655 words

Short running title: Parametric methods for ^{11}C-phenytoin

ABSTRACT

In this study the performance of various methods for generating quantitative parametric images of dynamic ^{11}C-phenytoin PET studies will be evaluated. **Methods:** Double baseline 60 min dynamic ^{11}C-phenytoin PET studies, including online arterial sampling, were acquired for 6 healthy subjects. Parametric images were generated using Logan plot analysis, a basis function method (BFM) and spectral analysis (SA). Parametric distribution volume (V_T) and influx rate (K_1) were compared to those obtained from non-linear regression (NLR) analysis of time activity curves. In addition, global and regional test-retest (TRT) variability was determined for parametric K_1 and V_T values. **Results:** Biases in V_T observed with all parametric methods were less than 5%, For K_1, SA showed negative bias of 16%. Mean TRT variabilities of V_T and K_1 were less than 10% for all methods. Shortening the scan duration to 45 min provided similar V_T and K_1 with comparable TRT performance compared to 60 min data. **Conclusions:** Among the various parametric methods tested, BFM provided parametric V_T and K_1 values with the least bias compared to NLR data and showed TRT variabilities lower than 5%, also for smaller volume of interest (VOI) sizes (i.e. higher noise levels) and shorter scan duration.

Key Words: ^{11}C-phenytoin, PET quantification, parametric kinetic modelling, test-retest variability

INTRODUCTION

It has been proposed that P-glycoprotein (P-gp) may play a role in treatment-resistant central nervous system disorders *(1)*. P-gp is an ATP-binding cassette transmembrane glycoprotein located at the luminal side of the blood brain barrier, where it functions as an efflux transporter and hence prevents its substrates from entering the brain. In common central nervous system disorders, such as epilepsy, overexpression of P-gp is thought to be an important mechanism of pharmacoresistance *(2,3)*.

At present, several ^{11}C labelled P-gp substrate tracers are available, which are promising imaging tools for *in vivo* assessment of P-gp function at the blood brain barrier. The best characterised tracers are (*R*)-^{11}C-verapamil *(4-7)* or ^{11}C-N-desmethylloperamide (^{11}C-dLop) *(8)*. In addition, tracers to measure P-gp expression, such as ^{11}C-laniquidar *(9-11)* and ^{11}C-tariquidar *(12)*, are available.

In principle, mapping of the P-gp distribution using positron emission tomography (PET) can also be performed using relatively weak P-gp substrate tracers, as these should yield higher cerebral uptake than strong substrate tracers, such as (*R*)-^{11}C-verapamil *(7)*. Phenytoin is a weak P-gp substrate and, in a previous study, a reversible single tissue compartment model with blood volume parameter (1T2k+V_b) was identified as the best candidate model for describing ^{11}C-phenytoin kinetics in normal subjects *(13)*. ^{11}C-phenytoin showed a number of potential advantages, such as low metabolism, lower efflux rate (k_2) than e.g. ^{11}C-verapamil, and the ability to shorten scan duration from 60 to 45 min without notable loss of accuracy and precision of the pharmacokinetic parameters *(13)*.

To study differences in P-gp function at the voxel level parametric ^{11}C-phenytoin images may be needed. To date, no parametric methods have been applied to ^{11}C-phenytoin data yet. Therefore, the aim of the present study was to investigate the performance of various parametric methods for describing ^{11}C-phenytoin kinetics.

MATERIALS AND METHODS

Scanning protocol

A total of six healthy male volunteers (mean age 28 years, range 21 to 32 years) were included in this study. All subjects were screened for medical history and underwent physical (including neurological) examination and laboratory tests. Subjects were also screened for neurological and psychiatric illness and history of drug abuse. Written informed consent was obtained from each subject after giving a written and verbal description of the study. The study was approved by the Medical Ethics Review Committee of the VU University Medical Center.

All subjects underwent two baseline dynamic PET studies on the same day. Scans were performed on a Gemini TF PET/CT scanner (Philips Medical Systems). The properties of this scanner have been reported elsewhere *(14)*. Prior to tracer injection, a low-dose computed tomograph scan was performed. These data were used to correct the subsequent emission scan for photon attenuation. Next, a dynamic emission scan in 3D acquisition mode was started simultaneously with an intravenous injection of 345 ± 54 (mean ± standard deviation (SD)) MBq of ^{11}C-phenytoin with a specific activity of 72 ± 27 MBq·μmol^{-1}. ^{11}C-phenytoin was synthesized as described previously *(15)*. The radiotracer was provided in a total volume of 7 mL and

administered at a rate of 0.8 mL·s^{-1}, followed by a flush of 42 mL saline at 2.0 mL·s^{-1} using an infusion pump (Med-Rad).

During the 60 min ^{11}C-phenytoin scan, arterial blood was withdrawn continuously using an automatic on-line blood sampler (Veenstra Instruments) *(16)* at a rate of 5 mL·min^{-1} for the first 5 min and 2.5 mL·min^{-1} thereafter. At 2.5, 5, 10, 20, 30, 40 and 60 min after tracer injection, continuous blood sampling was interrupted briefly to withdraw 7 mL manual blood samples. After each sample the arterial line was flushed with a heparinised saline solution. In addition, all subjects underwent a structural magnetic resonance imaging scan using a 1.5T Sonata scanner (Siemens Medical Solutions). More details on the study protocols can be found elsewhere *(13)*.

Blood and Image Analysis

Manual samples were used to determine plasma to whole blood radioactivity concentration ratios. In addition, concentrations of parent ^{11}C-phenytoin and its radioactive metabolites in plasma were determined using the described procedure in *(13)*. While for the image analysis, each MR image was co-registered with the corresponding PET image using VINCI software (Max Plank Institute). Next, VOI were defined using an automated method magnetic resonance imaging template based method (PVElab) *(17)*. The PgP is fairly uniformly distributed over the brain and therefore we used PVElab with the Hammers template that consisted of 67 regions covering the entire brain *(18)*. Grey and white matter segmentation of the co-registered MR image was performed using statistical parametric mapping version 8 (SPM8), which is incorporated in the PVElab software. These segmentations were used in combination

with the above mentioned VOI to extract grey matter regional values from the dynamic PET studies.

Parametric Analysis

Three different parametric methods were evaluated, the Logan plot analysis *(19)*, a BFM implementation of the single tissue compartment model with blood volume parameter *(20)* and SA *(21)*. For Logan, start and end times used were 12 and 140 min, respectively. For BFM method, the start and end basis function exponentials are 0.04 and 0.1 min^{-1} while for SA these are 0.03 and 0.17 min^{-1} respectively. Both methods were used with 30 basis functions.

The distribution volume (V_T) was obtained with all three methods, whilst the influx rate constant (K_1) was obtained using BFM and SA methods. The finding from this parametric studies will be compared with a previous NLR compartmental analysis performed on the same data *(13)*. Due to the sensitivity of NLR to noise, comparisons were performed at the VOI level with both small (≤ 5mL) and large (>5mL) volumes of interest to assess its effect on the test-retest variability of the studied parametric methods. After kinetic analysis, test-retest (TRT) variability of all kinetic parameters was calculated. TRT variability was calculated as the difference between test and retest kinetic parameters divided by their mean times 100%. Levene's test was used to assess the impact of different scan durations and VOI size on TRT of K_1 and V_T. In addition, the parametric V_T and K_1 values were averaged over each VOI. Test retest performance of VOI averaged parametric values was analysed using Bland–Altman plots *(22)*. Apart from assessing bias and impact of different VOIs sizes on parametric quantification, the impact of shorter scan duration on parametric test-retest variability was also studied.

RESULTS

Evaluation of bias between non-linear Regression and parametric methods

Typical ^{11}C-phenytoin parametric V_T and K_1 images for a healthy subject are shown in Supplemental Fig. 1. The correlations of V_T obtained using the three parametric methods with that obtained using NLR are shown in Fig. 1. Correlations are good for all 3 methods, but at the same time a small negative bias for the parametric methods of about 5% can be seen. Fig. 2 shows scatter plots of K_1 obtained using BFM and SA versus K_1 obtained using NLR. Correlation are excellent with an average overestimation of about 4% for BFM and an underestimation of about 16% for SA. Results from all correlation analyses are summarized in Table 1.

Test–Retest repeatability

Fig. 3 shows box plots of the percentage differences between test and retest values of V_T and K_1, respectively, obtained using Logan, BFM and SA methods. For each parametric method, results are provided for both small (≤5mL) and large (>5mL) VOIs. Repeatability of Logan and SA derived V_T seemed to be more affected by the use of small VOI BFM derived V_T. For K_1 both methods (BFM and SA) showed less than 5% (1 SD) TRT variability. In general, the median percentage difference between test and retest studies was about 5%. A somewhat wider range (larger inter-quartile range) in TRT variability of both K_1 and V_T (Fig. 3) was observed for small compared with large VOI, but this difference was not statistically significant (Levene's test, $p > 0.05$).

Impact of scan duration

Figs. 4A and 4B show V_T and K_1 TRT variability, respectively, for different scan durations. A somewhat wider range (larger inter-quartile range) of 9.3% for 30 min, versus 6.7 and 6.3 % for 45 and 60 min respectively in TRT variability of V_T. Logan and SA derived V_T seemed to be more affected by shortening the scan duration than BFM derived V_T. Yet, even for shorter scan durations, K_1 obtained with both methods (BFM and SA) showed less than 5% (1 SD) TRT variability. Shortening the scan duration to 45 min leads to slight deterioration of V_T TRT variability (from 1.7% to 2.1 for Logan, from 0.6 to 0.7 for BFM and 1.29 to 1.7 for SA), but differences were not statistically significant (Levene's test, $p > 0.05$). Differences between 45 min and 30 min scan durations (from 2.1% to 4% for Logan, from 0.7% to 0.75% for BFM and 1.7% to 2.9% for SA) however, were statically significant (Levene's test, $p<0.05$). TRT data are shown as Bland-Altman plots in Supplemental Fig 2 for 60 min of scan durations, while plot for 45 and 30 min are shown in Supplemental Figs. 3 and 4. Variabilities in the Bland-Altman plots for 45 min data were similar to those of 60 min data, but became larger for 30 min data. A summary of the Bland-Altman plots is given in Table 2. It can be seen that shortening the scan duration from 60 to 45 min did not substantially affect TRT variability of K_1 and V_T.

DISCUSSION

Results of the present study indicate the validity of several parametric methods for quantifying ^{11}C-phenytoin kinetics in the brain. Three well established and accurate parametric methods were evaluated. Other alternatives such as multi-linear analysis *(24)* were not available at our institute and could not be evaluated in the current study. However, it should be noted that this method could provide improved calculation time compared with BFM because of full linear approach. For V_T, strong correlations and good agreement were seen between the various parametric methods and NLR. The small negative bias of about -5% was mainly caused by the data from a single subject (p5). Unfortunately, it was not possible to identify any reason for this discrepancy. Although the Logan plot does not take blood volume (V_b) into account, the bias in V_T was not substantially different from that biases seen with BFM and SA. In addition, although Logan plot analysis may suffer from noise induced bias *(23,24)*, this was not seen in the present study. BFM showed an overestimation in K_1 of about 4% with a larger underestimation in case of SA. The incorporation of V_b as a fit parameter would result in an underestimation of K_1 for SA (Fig. 2). Therefore, the SA analysis was repeated without incorporating V_b as fit parameter. In this case the underestimation in K_1 reduced to about 5%. At the same time, however, bias in V_T increased to about 15%. Overall, amongst the three parametric methods, BFM provided the smallest bias in V_T of 5% underestimation compared to NLR.

As shown in Fig. 3, the TRT variabilities of V_T and K_1 for all three parametric methods were small (SD <5%). Overall, BFM shows the best TRT variability for V_T, followed by SA and Logan, respectively. With respect to K_1, SA seemed to provide better TRT variability than BFM. TRT variabilities were slightly increased for small compared to large VOI for all parametric methods. In addition, the TRT percentage of V_T and K_1 in parametric methods are comparable to

NLR method. Even though the TRT variabilities were small, there might be a limitation for quantification of ^{11}C-phenytoin in or near high uptake regions such as the choroid plexus due to spill over effects as was also seen for the hippocampus in (*R*)-^{11}C-verapamil studies *(25)*.

In general TRT variabilities of K_1 and V_T increased when shortening the scan duration. V_T repeatability obtained with BFM seemed to be less affected when shortening scan duration. K_1 repeatability was more sensitive to reducing scan duration. Overall, scan duration could be shortened from 60 to 45 min without substantially affecting V_T and K_1 repeatability for any of the methods tested. The performances of various methods, however, were solely based on data obtained from healthy (male) subjects. Further studies will be needed to assess whether various parametric method are sensitive enough to provide better quantification under other and/or pathological conditions.

Overall, from our studies the finding shows that the BFM seems to be a good parametric method for the evaluation of ^{11}C-phenytoin studies with potential to reduce the scan duration to 45 min.

CONCLUSIONS

Amongst the different parametric methods for quantifying ^{11}C-phenytoin kinetics in the brain, BFM produced the best results in term of bias and repeatability. In addition, scan duration could be shortened to 45 min, but further validation under pathological conditions is warranted.

Disclosure/ Conflict of Interest

The authors declare that they have no competing interests.

Reference List

(1) Loscher W, Potschka H. Blood-brain barrier active efflux transporters: ATP-binding cassette gene family. *NeuroRx.* 2005; 2:86-98.

(2) Dombrowski SM, Desai SY, Marroni M, et al. Overexpression of multiple drug resistance genes in endothelial cells from patients with refractory epilepsy. *Epilepsia.* 2001; 42:1501-1506.

(3) Langer O, Bauer M, Hammers A, et al. Pharmacoresistance in epilepsy: a pilot PET study with the P-glycoprotein substrate R-[(11)C]verapamil. *Epilepsia.* 2007; 48:1774-1784.

(4) Bart J, Willemsen AT, Groen HJ, et al. Quantitative assessment of P-glycoprotein function in the rat blood-brain barrier by distribution volume of [11C]verapamil measured with PET. *Neuroimage.* 2003; 20:1775-1782.

(5) Sasongko L, Link JM, Muzi M, et al. Imaging P-glycoprotein transport activity at the human blood-brain barrier with positron emission tomography. *Clin Pharmacol Ther.* 2005; 77:503-514.

(6) Syvanen S, Hammarlund-Udenaes M. Using PET studies of P-gp function to elucidate mechanisms underlying the disposition of drugs. *Curr Top Med Chem.* 2010; 10:1799-1809.

(7) Feldmann M, Asselin MC, Liu J, et al. P-glycoprotein expression and function in patients with temporal lobe epilepsy: a case-control study. *Lancet Neurol.* 2013; 12:777-785.

(8) Langer O, Bauer M, Hammers A, et al. Pharmacoresistance in epilepsy: a pilot PET study with the P-glycoprotein substrate R-[(11)C]verapamil. *Epilepsia.* 2007; 48:1774-1784.

(9) Luurtsema G, Verbeek GL, Lubberink M, et al. Carbon-11 labeled tracers for in vivo imaging P-glycoprotein function: kinetics, advantages and disadvantages. *Curr Top Med Chem.* 2010; 10:1820-1833.

(10) Moerman L, Dumolyn C, Boon P, De VF. The influence of mass of [11C]-laniquidar and [11C]-N-desmethyl-loperamide on P-glycoprotein blockage at the blood-brain barrier. *Nucl Med Biol.* 2012; 39:121-125.

(11) Froklage FE, Boellaard R, Bakker E, et al. Quantification of 11C-laniquidar kinetics in the brain. *J Nucl Med.* 2015; 56:1730-1735.

(12) Bauer F, Kuntner C, Bankstahl JP, et al. Synthesis and in vivo evaluation of [11C]tariquidar, a positron emission tomography radiotracer based on a third-generation P-glycoprotein inhibitor. *Bioorg Med Chem.* 2010; 18:5489-5497.

(13) Mansor MS, Boellaard R, Froklage FE, et al. Quantification of dynamic 11C-Phenytoin PET studies. *J Nucl Med.* 2015; 56:1372-1377.

(14) Surti S, Kuhn A, Werner ME, et al. Performance of Philips Gemini TF PET/CT scanner with special consideration for its time-of-flight imaging capabilities. *J Nucl Med.* 2007; 48:471-480.

(15) Verbeek J, Eriksson J, Syvanen S, et al. [11C]phenytoin revisited: synthesis by [11C]CO carbonylation and first evaluation as a P-gp tracer in rats. *EJNMMI Res.* 2012; 2:36.

(16) Boellaard R, van LA, van Balen SC, Hoving BG, Lammertsma AA. Characteristics of a new fully programmable blood sampling device for monitoring blood radioactivity during PET. *Eur J Nucl Med.* 2001; 28:81-89.

(17) Svarer C, Madsen K, Hasselbalch SG, et al. MR-based automatic delineation of volumes of interest in human brain PET images using probability maps. *Neuroimage.* 2005; 24:969-979.

(18) Hammers A, Koepp MJ, Free SL, et al. Implementation and application of a brain template for multiple volumes of interest. *Hum Brain Mapp.* 2002; 15:165-174.

(19) Logan J, Fowler JS, Volkow ND, et al. Graphical analysis of reversible radioligand binding from time-activity measurements applied to [N-11C-methyl]-(-)-cocaine PET studies in human subjects. *J Cereb Blood Flow Metab.* 1990; 10:740-747.

(20) Gunn RN, Gunn SR, Turkheimer FE, Aston JA, Cunningham VJ. Positron emission tomography compartmental models: a basis pursuit strategy for kinetic modeling. *J Cereb Blood Flow Metab.* 2002; 22:1425-1439.

(21) Cunningham VJ, Jones T. Spectral analysis of dynamic PET studies. *J Cereb Blood Flow Metab.* 1993; 13:15-23.

(22) Martin Bland J, Altman D. Statistical methods for assessing agreement between two methods of clinical measurement. *The Lancet.* 1986; 327:307-310.

(23) Slifstein M, Laruelle M. Effects of statistical noise on graphic analysis of PET neuroreceptor studies. *J Nucl Med.* 2000; 41:2083-2088.

(24) Ichise M, Toyama H, Innis RB, Carson RE. Strategies to improve neuroreceptor parameter estimation by linear regression analysis. *J Cereb Blood Flow Metab.* 2002; 22:1271-1281.

(25) Bauer M, Karch R, Neumann F, et al. Assessment of regional differences in tariquidar-induced P-glycoprotein modulation at the human blood-brain barrier. *J Cereb Blood Flow Metab.* 2010; 30:510-515.

FIGURES

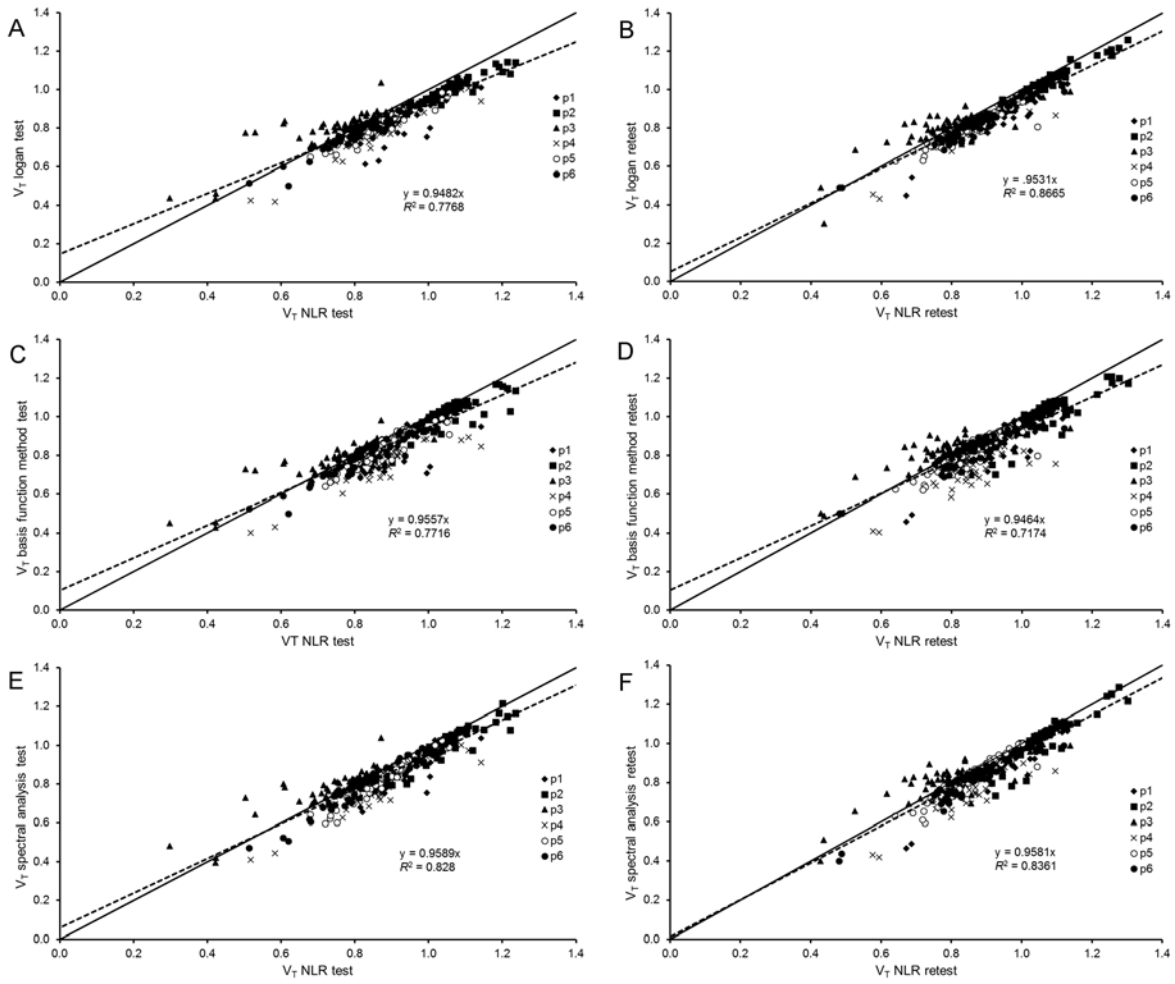

Figure 1. Scatter plots of regional averaged V_T obtained with the parametric method versus NLR analysis, pooled over six subjects. **A)** V_T using Logan for test **B)** Logan retest **C)** BFM test **D)** BFM retest **E)** SA test and **F)** SA retest. The solid line represents the line of identity, while dotted line represents the correlation line with intercept. Data were taken from whole regions.

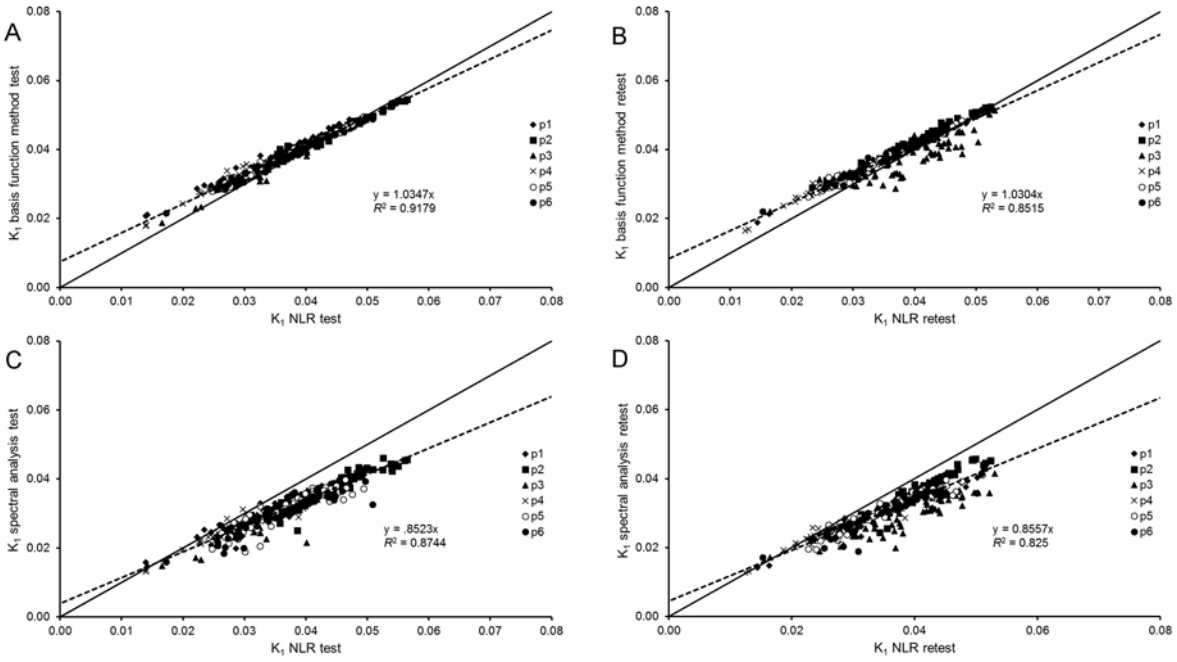

Figure 2. Scatter plots of K_1 obtained with the parametric method versus NLR analysis pooled over six subjects. **A)** K_1 using BFM for test **B)** BFM retest **C)** SA test **D)** SA retest. Solid line represents the line of identity, while dotted line represents the correlation line with intercept.

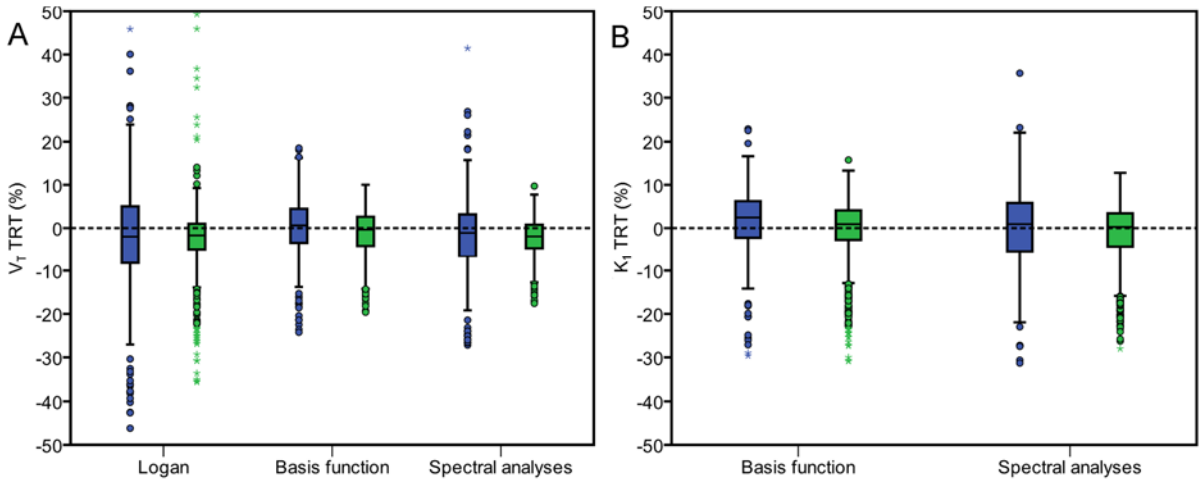

Figure 3. Test-retest variability of **(A)** V_T and **(B)** K_1 for different parametric methods for small (≤5mL, blue) and large (>5mL, green) volumes of interest.

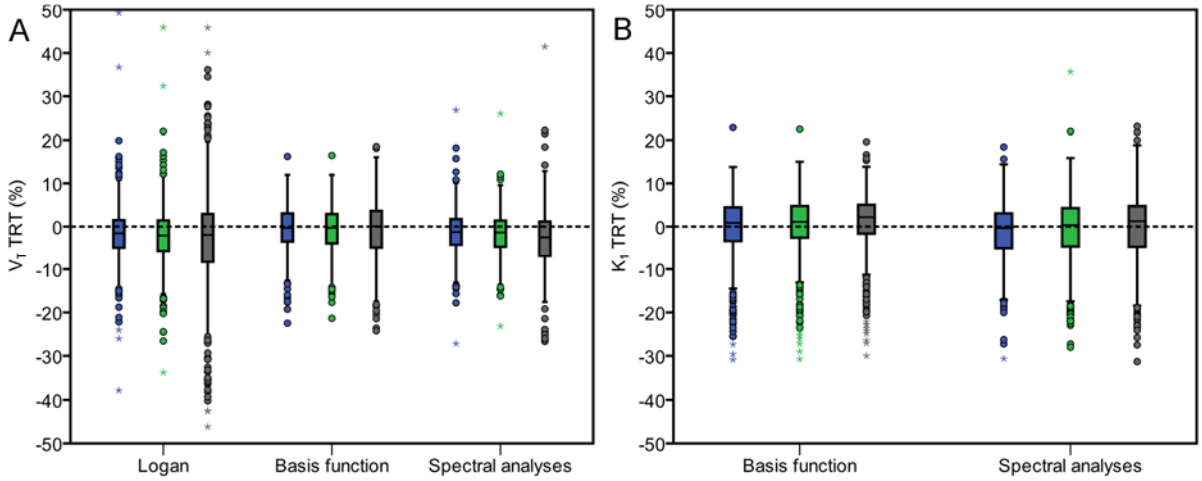

Figure 4. Test-retest variability of V_T **(A)** and K_1 **(B)** for different parametric methods and scan durations. The blue colour boxplot represent the 60 min, green and brown represent 45 and 30 min respectively.

TABLES

Table 1. Summary of correlation, slope and intercept between various parametric methods compared with NLR.

	Correlation (R^2)	slope	intercept	Correlation (R^2) with zero intercept	Slope with zero intercept
Logan V_T test	0.81	0.79	1.45×10^{-1}	0.78	0.95
Logan V_T retest	0.87	0.90	5.30×10^{-2}	0.87	0.95
BFM V_T test	0.79	0.84	1.03×10^{-1}	0.77	0.96
BFM V_T retest	0.73	0.83	1.05×10^{-1}	0.72	0.95
SA V_T test	0.83	0.89	5.95×10^{-2}	0.83	0.96
SA V_T retest	0.84	0.94	1.34×10^{-2}	0.84	0.96
BFM K_1 test	0.97	0.84	7.40×10^{-3}	0.92	1.03
BFM K_1 retest	0.92	0.81	8.30×10^{-3}	0.85	1.03
SA K_1 test	0.89	0.75	3.90×10^{-3}	0.87	0.85
SA K_1 retest	0.85	0.74	4.60×10^{-3}	0.83	0.86

NLR, non-linear regression method; BFM, basic function method; SA, spectral analysis; V_T, distribution volume; K_1, influx rate constant

Table 2. Summary of the results for Bland-Altman plots for each method with different scan durations for V_T (Logan, BFM and SA) and K_1 (BFM and SA).

	Mean	SD	Lower limit (-1.96SD)	Upper Limit (+1.96SD)
Logan V_T 60 min	-1.64×10^{-2}	5.17×10^{-2}	-1.18×10^{-1}	8.49×10^{-2}
BFM V_T 60 min	-5.54×10^{-3}	4.08×10^{-2}	-8.54×10^{-2}	7.43×10^{-2}
SA V_T 60 min	4.39×10^{-2}	-1.22×10^{-2}	-9.81×10^{-2}	7.38×10^{-2}
Logan V_T 45 min	-1.87×10^{-2}	5.50×10^{-2}	-1.26×10^{-1}	8.91×10^{-2}
BFM V_T 45 min	-6.66×10^{-3}	4.22×10^{-2}	-8.93×10^{-2}	7.60×10^{-2}
SA V_T 45 min	-1.33×10^{-2}	4.35×10^{-2}	-9.86×10^{-2}	7.19×10^{-2}
Logan V_T 30 min	-3.48×10^{-2}	1.24×10^{-1}	-2.78×10^{-1}	2.08×10^{-1}
BFM V_T 30 min	-5.81×10^{-3}	5.41×10^{-2}	-1.12×10^{-1}	1.00×10^{-1}
SA V_T 30 min	-1.88×10^{-2}	4.72×10^{-2}	-1.11×10^{-1}	7.36×10^{-2}
BFM K_1 60 min	-1.71×10^{-4}	2.80×10^{-3}	-5.66×10^{-3}	5.31×10^{-3}
SA K_1 60 min	2.08×10^{-3}	-3.91×10^{-4}	-4.46×10^{-3}	3.68×10^{-3}
BFM K_1 45 min	-5.76×10^{-5}	2.82×10^{-3}	-5.58×10^{-3}	5.46×10^{-3}
SA K_1 45 min	-3.14×10^{-4}	2.08×10^{-3}	-4.39×10^{-3}	3.76×10^{-3}
BFM K_1 30 min	2.35×10^{-4}	2.88×10^{-3}	-5.41×10^{-3}	5.88×10^{-3}
SA K_1 30 min	-1.30×10^{-5}	2.18×10^{-3}	-4.29×10^{-3}	4.26×10^{-3}

BFM, basic function method; SA, spectral analysis; V_T, distribution volume; K_1, influx rate constant